HAL
open science

Functional role of the Werner syndrome RecQ helicase in human fibroblasts

Kiranjit K. Dhillon, Julia Sidorova, Yannick Saintigny, Martin Poot, Katherine Gollahon, Peter S. Rabinovitch, Raymond J. Monnat Jr

To cite this version:

Kiranjit K. Dhillon, Julia Sidorova, Yannick Saintigny, Martin Poot, Katherine Gollahon, et al.. Functional role of the Werner syndrome RecQ helicase in human fibroblasts. Aging Cell, 2007, 6 (1), pp.53 - 61. 10.1111/j.1474-9726.2006.00260.x . cea-01938071

HAL Id: cea-01938071

https://cea.hal.science/cea-01938071v1

Submitted on 28 Nov 2018

HAL is a multi-disciplinary open access archive for the deposit and dissemination of scientific research documents, whether they are published or not. The documents may come from teaching and research institutions in France or abroad, or from public or private research centers.

L'archive ouverte pluridisciplinaire **HAL**, est destinée au dépôt et à la diffusion de documents scientifiques de niveau recherche, publiés ou non, émanant des établissements d'enseignement et de recherche français ou étrangers, des laboratoires publics ou privés.

Aging Cell (2007) **6**, pp53–61 Doi: 10.1111/j.1474-9726.2006.00260.x

Functional role of the Werner syndrome RecQ helicase in human fibroblasts

Kiranjit K. Dhillon,[1,2]* Julia Sidorova,[1]* Yannick Saintigny,[1]*† Martin Poot,[1]*† Katherine Gollahon,[1] Peter S. Rabinovitch[1] and Raymond J. Monnat, Jr[1,2]

Departments of [1]Pathology and [2]Genome Science, University of Washington, Seattle, WA 98195-7705, USA

Summary

Werner syndrome is an autosomal recessive human genetic instability and cancer predisposition syndrome that also has features of premature aging. We focused on two questions related to Werner syndrome protein (WRN) function in human fibroblasts: Do WRN-deficient fibroblasts have a consistent cellular phenotype? What role does WRN play in the recovery from replication arrest? We identified consistent cell proliferation and DNA damage sensitivity defects in both primary and SV40-transformed fibroblasts from different Werner syndrome patients, and showed that these defects could be revealed by acute depletion of WRN protein. Mechanistic analysis of the role of WRN in recovery from replication arrest indicated that WRN acts to repair damage resulting from replication arrest, rather than to prevent the disruption or breakage of stalled replication forks. These results identify readily quantified cell phenotypes that result from WRN loss in human fibroblasts; delineate the impact of cell transformation on the expression of these phenotypes; and define a mechanistic role for WRN in the recovery from replication arrest.

Key words: DNA repair; DNA replication; homologous recombination; premature aging; RecQ helicase; Werner syndrome.

Introduction

Werner syndrome (WS) is an autosomal recessive human genetic instability and cancer predisposition syndrome with features of premature aging. WS patients begin to develop the appearance of premature aging as young adults, together with an increased risk of age-associated diseases such as cancer, atherosclerotic vascular disease, diabetes mellitus, and osteoporosis (Epstein *et al*., 1966; Goto, 1997). The resemblance of WS to accelerated normal aging has focused attention on understanding the molecular and cellular basis of WS. The presumption is that a deep understanding of WRN function at the cellular and organismal level will provide useful mechanistic insights into the biology of aging and the pathogenesis of clinically important, age-associated diseases (Kipling *et al*., 2004; Monnat & Saintigny, 2004).

The *WRN* gene was identified by positional cloning in 1996, and found to encode a member of the human RecQ helicase protein family (WRN or RECQL2; Yu *et al*., 1996). Two other human RecQ helicase deficiency syndromes are also genetic instability and cancer predisposition syndromes. Loss of BLM or RECQL3 results in Bloom syndrome (Ellis *et al*., 1995), while mutations in *RECQL4* lead to Rothmund–Thomson syndrome with a high risk of osteosarcoma (Kitao *et al*., 1999; Wang *et al*., 2003). RecQ helicases appear to regulate genome stability and cell viability in many organisms (Hickson, 2003; Khakhar *et al*., 2003; Opresko *et al*., 2004a). However, it is not clear how these effects are mediated, or whether they involve common mechanistic pathways in different organisms.

Cellular defects in WS were first identified in fibroblasts (Epstein *et al*., 1966; Martin *et al*., 1970), and it appears that fibroblasts and other mesenchymal cell lineages may be particularly sensitive to the loss of WRN function (Epstein *et al*., 1966; Masuda *et al*., 2001; Monnat & Saintigny, 2004). The presence of chromosomal translocations, deletions and re-arrangements in primary WS fibroblast and lymphocyte cultures led to the suggestion that WS was a chromosomal instability syndrome (Hoehn *et al*., 1975; Salk *et al*., 1985), and that the cellular phenotype of WS might be an expression of constitutive genomic instability. Subsequent analyses revealed that the chromosomal instability of WS cells could be accentuated by DNA damage (Gebhart *et al*., 1988), and that WRN-deficient cells were selectively sensitive to killing by 4-nitroquinoline 1-oxide (4-NQO; Gebhart *et al*., 1985; Ogburn *et al*., 1997; Prince *et al*., 1999; Hisama *et al*., 2000); by camptothecin, a DNA topoisomerase I inhibitor (Okada *et al*., 1998; Poot *et al*., 1999); and most notably and strongly by DNA cross linking drugs such as *cis*-platinum (*cis*-Pt), mitomycin-C, or 8-methoxypsoralen + UV light (8-MOP+UV; Poot *et al*., 2001, 2002a).

In order to better understand WRN function in human cells, we systematically analyzed cell proliferation, DNA damage sensitivity and homology-dependent recombination in primary and SV40-transformed WS fibroblasts. We also determined

*These authors contributed equally to the work described here.
†Present address: LMR-UMR, CEA/CNRS, 217, 92265 Fontenay aux Roses Cedex France.
‡Present address: UMC Utrecht, Section for Molecular Cytogenetics and Genome Science, PO Box 85090, Mailstop KC02.084.2, 3508 AB Utrecht, The Netherlands.
Correspondence
Raymond J. Monnat, Jr, Department of Pathology, Box 357705, University of Washington, Seattle, WA 98195-7705, USA. Tel.: 206 616 7392; fax: 206 543 3967; e-mail: monnat@u.washington.edu

Accepted for publication *6 October 2006*

© 2006 The Authors
Journal compilation © Blackwell Publishing Ltd/Anatomical Society of Great Britain and Ireland 2006

which of these measures could be modified or revealed by acute depletion of WRN. Finally, we analyzed the mechanistic role of WRN in the recovery from DNA replication arrest. The results of these experiments identify consistent, readily quantified cell phenotypes that accompany WRN loss, and provide new information on the mechanistic origin of these phenotypes in human fibroblasts.

Results

WS fibroblasts display consistent cell proliferation and cell survival defects

We used complementary colony-size distribution (CSD; Smith *et al*., 1978), colony-forming efficiency (CFE) and proliferative survival (Poot *et al*., 2002b) assays to analyze the survival and proliferation of primary and SV40-transformed fibroblasts that had been mutation typed and shown to lack WRN protein (Prince *et al*., 1999; Moser *et al*., 2000; Huang *et al*., 2006; additional results not shown). Primary WS fibroblasts showed a marked reduction in median colony cell number in CSD assays as well as a reduced CFE in the absence of exogenous DNA damage. These measures were not sensitive to growth interval, and thus reflect an intrinsic reduction in cell division probability of WRN-deficient fibroblasts. This proliferation defect could be further accentuated by DNA damaging agents such as *cis*-Pt that selectively kill WRN-deficient cells in a dose- and exposure time-dependent manner (Fig. 1a; Poot *et al*., 1999, 2002a; Saintigny *et al*., 2002; additional results not shown). The proliferative survival of two of three WS cell strains over 72 h after 8-MOP+UV damage was also markedly suppressed as compared with controls (Supplementary Fig. S1). 8-MOP preferentially forms DNA-interstrand cross links after UV irradiation (Hearst *et al*., 1984). These results document the presence of a proliferative defect and DNA cross-link sensitivity in primary WS fibroblasts that is not suppressed by SV40 transformation (Saintigny *et al*., 2002).

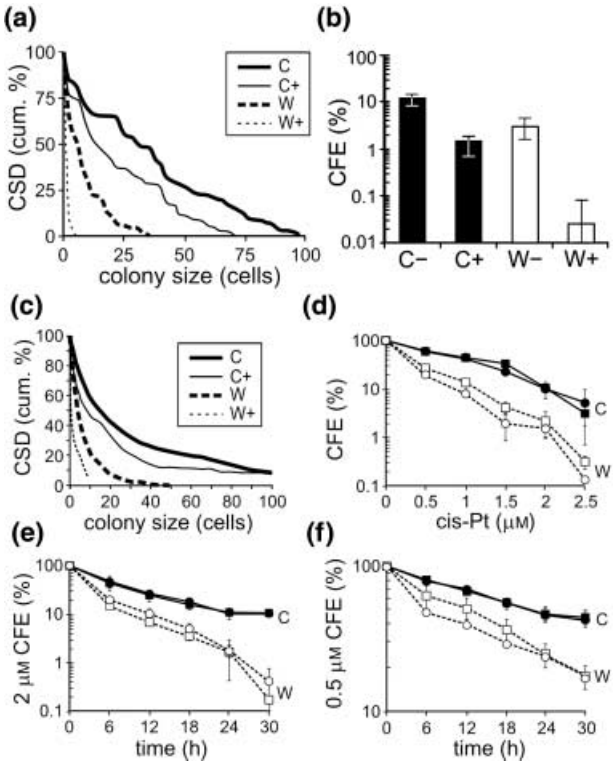

Fig. 1 WS fibroblasts have a cell proliferation defect and DNA cross link sensitivity. (a) Cumulative colony-size distributions (CSD) of passage level-matched control fibroblast strain 88-1 (solid lines) and of WS fibroblast strain 73-24 (dashed lines) and prior to or after (+) 2 μM *cis*-Pt for 24 h. (b) Colony-forming efficiency (CFE) of the same control and WS fibroblast strains prior to and after 2 μM *cis*-Pt for 24 h. (c) CSD's of SV40-transformed control fibroblast cell line GM639 (solid lines) and WS fibroblast cell line WV1 (dashed lines) before (bold lines) and after 2 μM *cis*-Pt for 24 h. (d) CFE's of control fibroblast cell lines GM639 (filled boxes) and GM847 (filled circles) and of WS fibroblast cell lines WV1 (open boxes) and AG11395 (open circles) as a function of *cis*-Pt dose for 24 h, or as a function of time of treatment with 2 μM (e) or 0.5 μM *cis*-Pt (f). Error bars in panels indicate standard deviations from 2 to > 4 replicate experiments per cell line, time point and dose.

Acute WRN depletion reveals WS cellular phenotype

In order to better define the WS cell phenotype in an isogenic background, we characterized the phenotype of primary and SV40-transformed control (WRN+) fibroblasts after acute WRN depletion. This approach has the virtue of starting with WRN+ control cells, which minimizes changes due to genomic instability in WRN-deficient cells and, thus, has the potential to more directly reveal the consequences of WRN loss. WRN depletion from primary and SV40-transformed control fibroblasts was mediated by retroviral expression of a WRN-targeted short hairpin RNA (shRNA; Grandori *et al*. 2003). Western blot analysis was used to determine the time course of WRN depletion, which was nearly complete for both SV40-transformed and primary fibroblasts: 93 to 99% depletion from SV40 fibroblasts over days 4–15 after shRNA expression (Fig. 2a), and up to 95% depletion from primary fibroblasts over days 4–11 after shRNA expression vs. either a vector-only control or a scrambled sequence control shRNA (additional data not shown). The half-life of WRN protein in these experiments, estimated from a simple first order exponential decay model, was ~19 h for SV40 fibroblasts and ~54 h for primary fibroblasts. Our WRN half-life estimate for primary fibroblasts is virtually identical to the half-life that can be calculated from the data of Szekley *et al.* who transfected primary fibroblasts with a synthesized small interfering RNA (2005).

In order to determine cell survival and recombination in WRN-depleted fibroblasts we treated control SV40-transformed fibroblasts containing an integrated copy of the pNeoA recombination reporter plasmid (Fig. 2b) with 2 μM *cis*-Pt for 24 h on day 6, when ≤ 1% of wild-type WRN protein remained, and then determined cell survival and neo+ recombinant colony generation. WRN-depleted fibroblasts had a threefold reduction in cell survival as measured by CFE, and a fourfold reduction in the ability to generate recombination-dependent, G418-resistant

© 2006 The Authors
Journal compilation © Blackwell Publishing Ltd/Anatomical Society of Great Britain and Ireland 2006

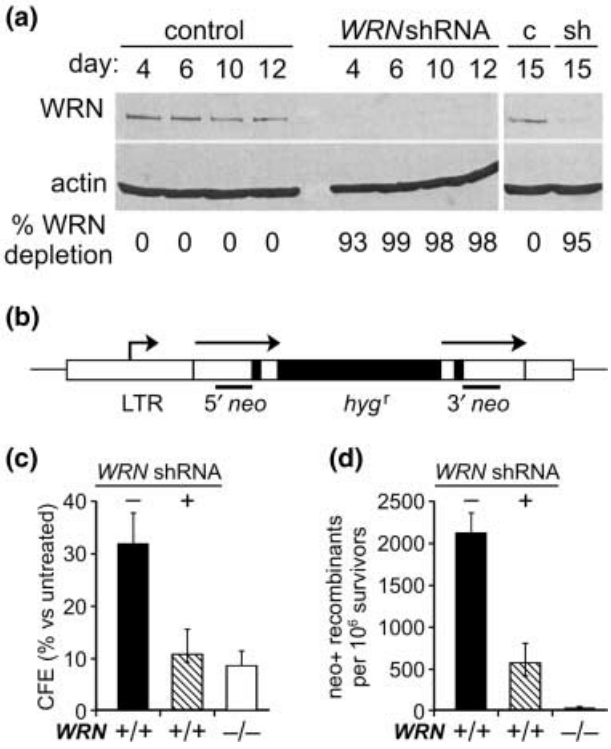

Fig. 2 WRN depletion from SV40 fibroblasts reveals a WS fibroblast phenotype. (a) Time course of short hairpin RNA (shRNA)-mediated WRN depletion from SV40-transformed control (WRN+) fibroblast cell line GM639-pNeoA vs. a vector-only control. Comparable results were obtained using a vector-only or scrambled sequence control shRNA (data not shown). (b) Structure of pNeoA mitotic recombination reporter plasmid. Recombination between genetically inactive copies of the neomycin phosphotransferase (*neo*) genes (→) generates a *neo*+ allele to permit growth in G418. Key: filled *neo* segments: inactivating linker insertions; solid underline: overlap region between linker insertion sites; LTR, long-terminal repeat; *hyg*^{r}, hygromycin-resistance gene. (c) Colony-forming efficiency (CFE) and (d) generation of G418-resistant cells 6 days after *cis*-Pt treatment of shRNA-mediated WRN depletion from GM639pNeoA SV40 fibroblasts (gray bar) vs. a vector-only control (filled bars). Treatment was 2 μM *cis*-Pt for 24 h. Open bars are survivals determined using SV40-transformed WS fibroblast cell AG11395 (Saito & Moses, 1991). Error bars represent the standard deviations of triplicate experiments.

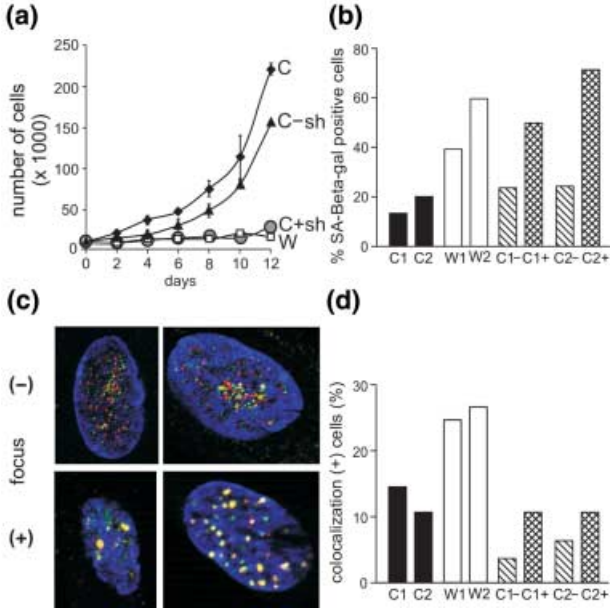

Fig. 3 WRN depletion from primary fibroblasts reveals a WS fibroblast phenotype. (a) Growth of control fibroblast cell strain 78-89 (c) over 12 days after retroviral expression of a *WRN*-targeted short hairpin RNA (shRNA) (C + sh) or transduction with a control retroviral vector (C – sh), as compared with primary WS fibroblast strain AG000780G (W). (b) Senescence-associated β-galactosidase-positive (SA-β-gal+) cells 7 days after WRN depletion, as compared with two vector-transduced control strains and two WS fibroblast strains (see cell strain key below). (c) Panels show representative cells scored as negative [upper panels (–)] or positive [lower panels (+)] for the presence of colocalization of γH2AX and pThr68-CHK2 in nuclear foci 7 days after shRNA-mediated WRN depletion. Large γH2AX foci virtually always colocalized with pThr68-CHK2-foci. (d) Percentage of focus-positive, colocalizing cells after 7 days of WRN depletion. An average of 146 cells per sample were counted (range 70–197 cells). Differences in frequency of focus (+) cells between WS and control cells were statistically significant in all pair wise comparisons (χ^2 values ≥ 5.5, $P \leq 0.02$ with 1 degree of freedom and Yates' correction). Both shRNA-depleted cell populations showed consistent increases in focus frequency, but did not reach statistical significance at the $P \leq 0.05$ level: $\chi^2 = 1.38$, $P \leq 0.3$ (C1 ± RNAi) and 2.63, $P \leq 0.11$ (C2 ± RNAi). Key: primary control human fibroblast cell strains were 71-95 (C1) and 78-89 (C2); primary WS fibroblast cell strains were 73-26 (W1) and AG000780G (W2).

(neo+) colonies as compared with controls (Fig. 2c,d). WRN depletion from primary fibroblasts was strongly growth suppressive, to a level comparable to that observed in primary WS fibroblasts (Fig. 3a). This proliferative defect was accompanied by an increase in the frequency of cells that stained for senescence-associated β-galactosidase (SA-β-gal) activity (Dimri *et al.*, 1995) to levels observed in primary WS fibroblast controls (Fig. 3b). Comparable results were observed in independent experiments that used primary fibroblast cell strains from two different donors (Fig. 3b).

In order to determine whether the growth suppression and increase in SA-β-gal+ primary fibroblasts was accompanied by an acute DNA damage response (d'Adda di Fagagna *et al.*, 2003; Szekely *et al.*, 2005), we immunostained cells to identify nuclear foci formed by the acute DNA damage markers γH2AX and phosphoThr68-CHK2 (Ahn *et al.*, 2004; Thiriet & Hayes, 2005). Co-immunostaining was used to identify cells in which the two proteins colocalized to form large nuclear foci. This provides a robust measure that is likely to be damage specific, and can be readily distinguished from small, spontaneous γH2AX foci that are often seen in the absence of exogenous DNA damage. There was a 2.5-fold increase in the frequency of cells containing one or more large γH2AX/pCHK2 focus after WRN depletion [Fig. 3c, bottom (+) panels], an increase comparable to that observed between control and WS fibroblast pairs (Fig. 3d). The lower absolute frequency of focus-positive cells in these experiments may be as a result of the retroviral transduction and selection protocol required to perform the assay. These acute depletion experiments demonstrate that cellular defects characteristic of WS primary fibroblasts can be revealed by the acute depletion of WRN protein from control primary and SV40 fibroblasts.

© 2006 The Authors
Journal compilation © Blackwell Publishing Ltd/Anatomical Society of Great Britain and Ireland 2006

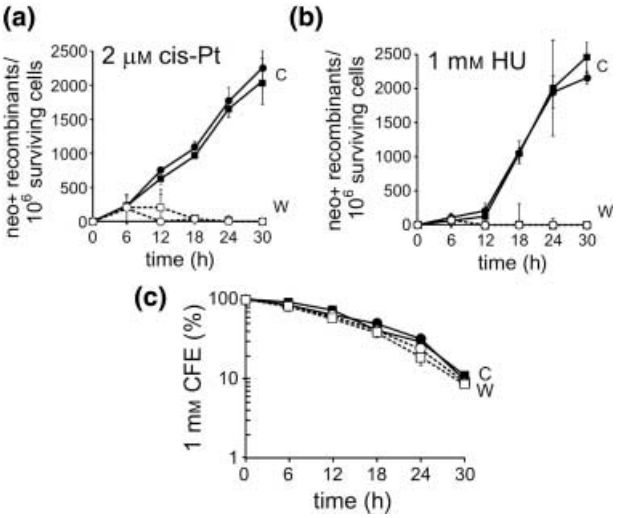

Fig. 4 Recombination defect in WS fibroblast cell lines after *cis*-Pt damage or replication arrest. (a) Generation of G418-resistant recombinant colonies per 10^6 surviving cells after treating WS and control SV40-transformed pNeoA recombination reporter cell line pairs with 2 μM *cis*-Pt for 6–30 h. (b) Generation of G418-resistant recombinant colonies per 10^6 surviving cells after treating cell lines with 1 mM hydroxyurea for 6–30 h followed by recovery. (c) Colony-forming efficiency of control and WS fibroblast cell line pairs after 1 mM hydroxyurea. Key: SV40-transformed control fibroblast cell lines GM847 (filled circles) and GM639 (filled boxes); WS fibroblast cell lines AG11395 (open circles) and WV1 (open boxes). Error bars in all panels represent the standard deviations of two to four replicate experiments per cell line, dose, and time point.

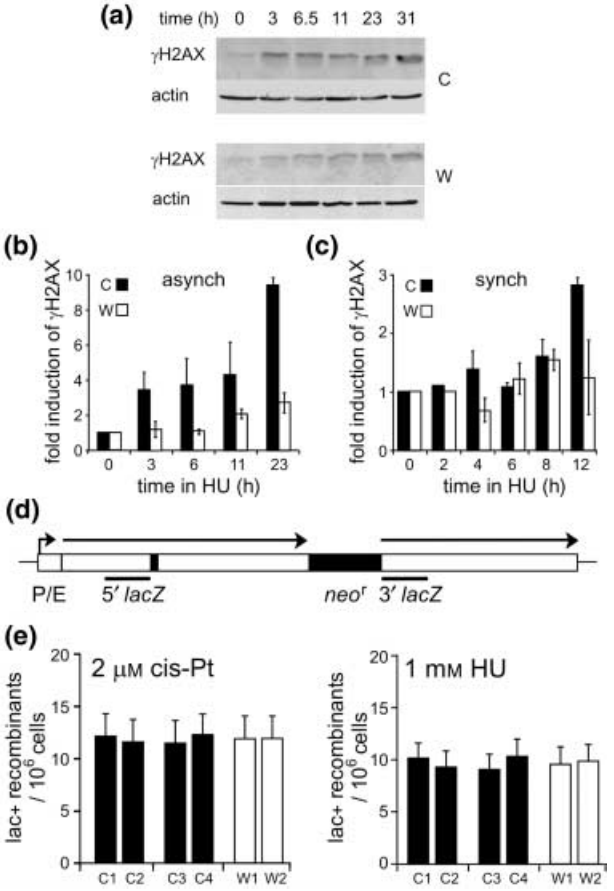

Fig. 5 WRN promotes repair of DNA damage generated by DNA damage or replication arrest. (a) γH2AX induction over 31 h after 1 mM hydroxyurea (HU)-mediated replication arrest in control (GM639, top panel) and in WS (WV1, bottom panel) SV40 fibroblast cell lines vs. a β-actin control. (b,c) γH2AX induction over 23 h after HU-mediated replication arrest in asynchronous cell cells (b) or over 12 h after HU-mediated replication arrest of mimosine-synchronized S-phase cells at 10–11 h after release (c). Cell lines were as in (a), error bars in both panels were standard deviations determined from three independent experiments, and γH2AX levels were normalized vs. actin and expressed as an 'n'-fold induction over base line determined prior to HU arrest. (d) Structure of the pLrec direct repeat *lacZ* recombination reporter plasmid (Herzing & Meyn, 1993): reporter genes (→) were inactivated by a linker insertion (5′ *lacZ*; filled box) or by an N-terminal deletion (3′ *lacZ*) and separated by a neomycin phosphotransferase (*neo*) gene. Regions of homology are underlined. P/E, promoter/enhancer. (e) Frequency of newly induced Lac+ cells per 10^6 surviving cells after treatment of WS or control cells with 2 μM *cis*-Pt for 24 h (left panel), or with 1 mM HU for 24 h (right panel). Error bars represent the standard deviations of two to four independent experiments per fibroblast subline. Cell line key: C1, 639L22; C2, 639Rec75; C3, LNL1; C4, 847L22; W1, WVP45; W2, WVP46 (Prince *et al.*, 2001).

Role of WRN in recovery from replication arrest

RecQ helicases have been proposed to play an important role in maintaining genomic stability and cell viability in response to replication arrest (Courcelle & Hanawalt, 1999; Doe *et al.*, 2000; Pichierri *et al.*, 2001; Oakley & Hickson, 2002). In order to further explore the role of WRN in replication arrest and recovery, we quantified DNA breakage, cell survival and the induction of recombination-dependent colony formation after reversible, hydroxyurea (HU)-mediated replication arrest. In contrast to *cis*-Pt damage, HU strongly induced recombinant colony formation only after 12 h or more of replication arrest. WS cells were profoundly recombination deficient at all time points after this 12-h 'silent interval' (Fig. 4a,b), a difference that cannot be explained by the differential killing of WS cells by HU (Fig. 4c). These results indicate that WRN is required for efficient recombinant colony generation, although not for fibroblast survival, after HU-mediated replication arrest.

In order to further elucidate the role of WRN in replication arrest recovery, we quantified DNA breakage and recombinant DNA molecule generation in WS and control SV40-transformed fibroblasts. We reasoned that if WRN acted early in replication arrest to stabilize or process replication forks, then WRN-deficient cells might show higher levels of DNA breakage and recombinant molecule formation in response to HU arrest. Conversely, if WRN acted late in recovery from replication arrest, then we anticipated seeing comparable levels of DNA breakage and recombinant molecule formation in WRN-deficient and control cells. DNA breakage in HU-arrested WS and control SV40 fibroblasts was quantified by Western blot analysis of γH2AX generation, a marker of DNA breakage.

The γH2AX content of asynchronous control cells rose 3–4-fold and remained at this level for up to 12 h of HU-mediated arrest, after which γH2AX levels rose to ~10-fold above baseline. The γH2AX content of WS cells, in contrast, did not rise in the initial 6 h after HU arrest and never rose to ≥ 3-fold above background after up to 24 h of HU arrest (Fig. 5a,b). Control

© 2006 The Authors
Journal compilation © Blackwell Publishing Ltd/Anatomical Society of Great Britain and Ireland 2006

cells have a higher S-phase fraction than do WS cells (50.6% for control cells over 24 h vs. 32.9% for WS cells; data not shown). Thus, in order to allow a direct comparison of DNA breakage in WS and control cells with comparable S-phase fractions, we repeated these experiments using mimosine-synchronized cell populations. When synchronized cultures were used, we observed no difference in γH2AX induction between WS and control cells over the first 8 h of HU arrest. At ≥ 12 h of arrest, control cells had a 2-fold higher level of γH2AX than did WS cells (Fig. 5c).

We observed no difference between WS and control fibroblasts in the generation of recombinant DNA molecules identified by β-galactosidase staining of pLrec cells (Fig. 5e). This is in contrast to the marked reduction in recombination-dependent, G418-resistant colony formation in WS, although not in control, pNeoA SV40 fibroblasts after *cis*-Pt damage or HU-mediated replication arrest (Fig. 4a,b). This apparent discrepancy in the behavior of the superficially similar pNeoA (Fig. 2b) and pLrec (Fig. 5d) recombination reporters is explained by different requirements of the two reporters to score recombinant events: pNeoA requires recombination and cell division to form recombinant G418-resistant colonies, while pLrec recombinants can be identified prior to, as well as after cell division by cytochemical staining for β-galactosidase activity. An analysis of spontaneous recombination in WS and control SV40 fibroblasts using pLrec and pNeoA, in which comparable results were obtained here, allowed us to identify a recombination defect in WS cells at resolution, when recombinant DNA molecules are topologically resolved and segregated to give rise to viable daughter cells (Prince *et al*., 2001).

The recombination reporter and γH2AX induction data shown in Figs 4 and 5 indicate that DNA breakage and DNA breakage-induced recombination is comparable in WS and control cells over 8–12 h after HU-mediated replication arrest. Moreover, the differential behavior of WS cells containing pNeoA or pLrec after HU-mediated replication arrest (cf. Fig. 4a,b with Fig. 5e) identify the same recombination resolution defect previously observed in WS for both spontaneous and *cis*-Pt-induced recombination (Prince *et al*., 2001; Saintigny *et al*., 2002).

Discussion

The cellular phenotype of WS has been most extensively studied in fibroblasts. This reflects the ease with which fibroblasts can be grown; early documentation of a proliferative defect in WS fibroblast cultures in conjunction with evidence for strong clonal succession (Epstein *et al*., 1966; Martin *et al*., 1970; Hoehn *et al*., 1975; Salk *et al*., 1981); and indications that fibroblasts and other mesenchymal cell lineages may be disproportionately affected in WS patients (Masuda *et al*., 2001).

Our experiments used complementary cell survival and proliferation assays to characterize the cell division defect of WS primary and SV40-transformed WS fibroblasts, and to demonstrate the selective sensitivity of primary and SV40-transformed WS fibroblasts to *cis*-Pt and to 8-MOP+UV light-mediated DNA damage (Fig. 1; Supplementary Fig. S1). Acute shRNA-mediated depletion of WRN, to levels observed in WS patient cells (≤ 5% of wild-type levels), was used to demonstrate that cell survival and recombination-dependent colony generation after *cis*-Pt damage depended directly upon WRN function (Fig. 2). In comparable experiments using primary fibroblasts, acute shRNA-mediated depletion of WRN was strongly growth suppressive and increased the frequency of cells expressing SA-β-gal activity and DNA damage-induced nuclear foci (Fig. 3). These results thus confirm and extend previous work from our and other laboratories (Grandori *et al*., 2003; Szekely *et al*., 2005), and delineate cellular phenotypes that result from acute WRN loss as opposed to secondary mutations or adaptation.

Many analyses of the WS cell phenotype have been performed using SV40-transformed fibroblasts. SV40 T antigen deregulates cell cycle entry to promote unscheduled DNA replication via its effects on Rb and p53, and may alter several cell cycle checkpoints (Ahuja *et al*., 2005). The persistence of constitutional genomic instability in SV40-transformed WS fibroblasts suggests that SV40 transformation confers a growth advantage on primary WS fibroblasts by suppressing the consequences of WRN loss, rather than by suppressing the constitutional genetic instability or DNA-damage sensitivity of primary WS cells (Fig. 1; Supplementary Fig. S1). Telomerase immortalization of WS fibroblasts, in contrast, suppresses both the 4-NQO sensitivity and cell proliferation defect of WS fibroblasts (Hisama *et al*., 2000; Wyllie *et al*., 2000). This appears to reflect important functional interactions between WRN and telomerase (see below). Thus, it is important to take into account the mechanism by which cell transformation modifies cell phenotype before drawing mechanistic conclusions about the underlying defect in WS cells.

WRN plays an important role in the postsynaptic or resolution phase of homology-dependent recombination (HDR; Prince *et al*., 2001; Saintigny *et al*., 2002), and maintains telomeres with the suppression of telomere sister chromatid exchanges and/or loss (Chang *et al*., 2004; Crabbe *et al*., 2004; Du *et al*., 2004; Opresko *et al*., 2004b; Laud *et al*., 2005). These observations suggest that there may be common substrates for WRN function in chromosomes and at telomeres such as 3-stranded DNA and, forked D- or T-loops that share common structures and are *in vitro* substrates for WRN (reviewed in Bachrati & Hickson, 2003; Opresko *et al*., 2004a, 2005). Work with human fibroblasts and in mouse models of WS indicate that short or critically short telomeres may trigger a requirement for WRN function (Chang *et al*., 2004; Crabbe *et al*., 2004; Du *et al*., 2004; Laud *et al*., 2005). These experiments also indicate that WRN function at telomeres may require only the helicase activity of WRN, in contrast to the role of WRN in HDR where the WRN exonuclease and helicase activities are both required (Bai & Murnane, 2003; Crabbe *et al*., 2004; Swanson *et al*., 2004; Laud *et al*., 2005).

WRN has long been suspected of playing a role in replication arrest recovery (Pichierri *et al*., 2001; Oakley & Hickson, 2002). The observation that HU-mediated replication arrest strongly induced recombination-dependent colony formation by control cells (although not by WS) provided a way to further explore this

© 2006 The Authors
Journal compilation © Blackwell Publishing Ltd/Anatomical Society of Great Britain and Ireland 2006

postulated role for WRN. Analysis of this HU-induced recombination defect of WS cells revealed no difference between WS and control cells in HU sensitivity, in DNA breakage or in the generation of recombinant DNA molecules after HU-mediated replication arrest (Figs 4 and 5). These data indicate that WRN likely acts late in replication arrest recovery, rather than early to limit DNA breakage or attenuate cell death. A late role for WRN in replication arrest recovery is thus consistent with the previously identified role of WRN in HDR, a repair pathway that can be used to fix DNA double strand breaks and restart disrupted replication forks (Prince *et al*., 2001; Oakley & Hickson, 2002; Saintigny *et al*., 2002; Helleday, 2003).

We observed no difference in the survival of WS and control fibroblast lineage cells in HU arrest-recovery experiments up to 30 h of HU arrest (Fig. 4c). This is in contrast to previous reports that ≥ 2 h of HU-mediated replication arrest rapidly and selectively killed WRN-deficient lymphoblastoid cell lines (Pichierri *et al*., 2001). One simple explanation for this difference is that lymphoblastoid cell lines are more likely to undergo apoptosis in response to DNA damage than are fibroblasts (see, for example, Poot *et al*., 2002a). Thus cell type- or cell lineage-specific effects may be important modifiers of the *in vivo* consequences of WRN loss of function.

How might the loss of WRN function in HDR or in telomere maintenance lead to the WS clinical phenotype? One likely explanation is that WRN loss promotes genetic instability, telomere shortening and cell loss in many cell lineages, with the progressive accumulation of mutant and senescent cells during adult life (Kipling *et al*., 2004; Monnat & Saintigny, 2004; Campisi, 2005; Herbig *et al*., 2006,Herbig & Sedivy, 2006). Fibroblasts and other mesenchymal lineage cells may be particularly sensitive to these consequences of WRN loss of function: they serve important mechanical and trophic functions in many tissues and organs; retain replicative potential throughout life; are refractory to damage-induced cell killing; and may be sensitive to both telomere loss-induced and telomere loss-independent senescence (Herbig *et al*., 2006; Herbig & Sedivy 2006). Thus several drivers of *in vivo* senescence in WS patients that could be exacerbated by DNA damage – genetic instability, mutation accumulation and increased cell loss – may be promoting the pathogenesis of cancer and other age-associated diseases in WS patients (Goto *et al*., 1996; Monnat, 2001, 2002).

Experimental procedures

Cells and cell culture

Primary WS and control fibroblast strains were isolated at the University of Washington (Seattle, WA, USA) or obtained from the Coriell Institute Cell Repositories (Camden, NJ, USA) and were *WRN* mutation typed by the Werner Syndrome International Registry (www.pathology.washington.edu/research/werner/ Huang *et al*., 2006). WS strains 73-24, 73-26, and AOMOR1010 were homozygous for an IVS25-1G>C mutation. Strain AG00780G was homozygous for a c.1336C>T mutation that lead to premature translation termination. Control fibroblast strains 71-95, 78-89, 88-1, and 82-6 have been previously described (Oshima *et al*., 1995; Poot *et al*., 2002a). SV40-transformed WS and control fibroblast cell lines were obtained from the Coriell Institute Cell Repositories or from Dr Robin Holliday (WS cell line WV1). WS cell line AG11395 was derived from WS fibroblast strain AG00780G (Saito & Moses, 1991). WS cell line WV1 (Huschtscha *et al*., 1986) contains a c.3004delG mutation that leads to a frameshift and premature translation termination of WRN. All cell strains or lines were grown as adherent monolayers in Dulbecco's modified minimal essential medium (DMEM) supplemented with 2 mM L-glutamine and 10% fetal bovine serum (Hyclone, Ogden, UT, USA) in a humidified 5% CO_2, 37 °C incubator. Cell lines were periodically screened to verify the absence of *Mycoplasma* infection by use of a polymerase chain reaction (PCR)-based screening assay.

Drugs and dyes

Stock solutions of *cis*-Pt (2 mM in 0.9% NaCl), hydroxyurea (1 M in phosphate-buffered saline) and 5-bromodeoxyuridine (BrdU; 10 mM in sterile water) were stored at –20 °C until use. Stocks of Hoechst 33258 (10 mM) and ethidium bromide (200 μg mL^{-1}) were prepared in sterile water and stored at 4 °C in the dark until use. Mimosine (10 mM) was prepared and stored in growth media at 4 °C until use. All chemicals were obtained from Sigma (St. Louis, MO, USA).

Cell growth, survival and recombination assays

Colony-size distribution and colony-forming efficiency assays were performed as previously described (Saintigny *et al*., 2002). Recombination frequency assays were performed as previously described (Prince *et al*., 2001; Saintigny *et al*., 2002). Newly induced Lac+ recombinant cells were identified by cytochemical staining of SV40 transformed WS or control fibroblast cell lines containing single integrated copies of the recombination reporter plasmid pLrec as previously described (Prince *et al*., 2001). The frequency of newly induced Lac+ cells was calculated by determining the difference in frequencies of Lac+ cells observed prior to and following treatment with 2 μM *cis*-Pt or 1 mM hydroxyurea.

Short hairpin RNA-mediated depletion of WRN

Depletion of WRN protein was achieved by retroviral expression of a WRN-targeted shRNA from the H1 RNA promoter of retroviral vector pBABEpuro as previously described (Grandori *et al*., 2003). Retrovirus was generated by transient transfection of 293T ΦNX amphotropic packaging cells. Control SV40-transformed fibroblasts (GM639pNeoA) transduced with pBABEpuro-shWRN, pBABEpuro vector, or a pBABEpuro vector expressing a scrambled sequence shRNA were placed on puromycin selection (1 μg mL^{-1}) at 48 h after infection. The estimated half-life of WRN was calculated using a simple

© 2006 The Authors
Journal compilation © Blackwell Publishing Ltd/Anatomical Society of Great Britain and Ireland 2006

first-order decay model from Western blot data of WRN protein content over the time course of depletion.

Western blot analyses

WRN depletion was quantified using whole cell extracts as previously described (Swanson *et al.*, 2004). Proteins were resolved on sodium dodecyl sulfate-polyacrylamide gel electrophoresis (SDS-PAGE), followed by immunoblotting using WRN-specific (BD Transduction Laboratories no. 611168) and actin-specific or GAPDH-specific loading control antibodies (Abcam Ltd., Cambridge, UK, ab6276 or ab9482, respectively). γH2AX protein content was determined by Western blot analysis of whole cell lysates that had been prepared by boiling cells in 1× Laemmli buffer for 10 min. Lysates were cleared by centrifugation, then separated by electrophoresis through 15% SDS-PAGE gels. Proteins were transferred onto nitrocellulose membrane (Bio-Rad, Richmond, CA, USA), blocked in TBS-T buffer containing 5% non-fat milk, then probed with mouse anti-γH2AX (Upstate no. 05-636) and mouse anti-actin antibodies (see above). Detection of bound antibodies was done using a horseradish peroxidase (HRP)-conjugated goat anti-mouse antibody (Southern Biotechnology 1070-01) and chemiluminescent detection (ECL, Amersham, UK). Data were visualized and quantified using a Storm Phosphorimager and ImageQuant software (Molecular Dynamics, Sunnyvale, CA, USA). In brief, signal intensities within lanes were corrected for lane- or band-specific background, and then normalized between lanes by use of actin or GAPDH loading controls.

Proliferative survival and cell-cycle distribution assays

Proliferative survival was determined by continuous BrdU labeling as previously described (Poot *et al.*, 2002b). Absolute cell numbers were determined by comparison with an internal chicken erythrocyte nucleus (CEN) standard. Cells were harvested by trypsinization, and combined with media containing floating cells. Cell pellets were resuspended in 0.5 mL FACS buffer (100 mM Tris-HCl pH 7.4, 154 mM NaCl, 1 mM $CaCl_2$, 0.5 mM $MgCl_2$, 0.2% bovine serum albumin, and 0.1% Nonident P-40) supplemented with 2 mM Hoechst 33258 and 15 000 CEN (Riese Enterprises, Grass Valley, CA, USA), then incubated for 15 min at room temperature. Ethidium bromide was added to a final concentration of 2 mM, followed by an additional 15-min incubation at room temperature in the dark. Fifty thousand particles (cells + CEN) were analyzed per sample with a Coulter Epics Elite (Beckman-Coulter Corporation, Fullerton, CA, USA) equipped with lasers for 10 mW UV and 15 mW 488 nm excitation.

Cell-cycle distributions were determined on cell aliquots that had been centrifuged and resuspended in buffer [146 mM NaCl, 10 mM Tris-HCl (pH 7.4), 2 mM $CaCl_2$, 22 mM $MgCl_2$, 0.01% bovine serum albumin, 0.1% nonidet P-40] supplemented with 10 $\mu g\ mL^{-1}$ 4,6′-diamidino-2-phenylindole (DAPI) and 10% (v/v) dimethyl sulfoxide prior to flow cytometry. Cell-cycle distributions were analyzed using MCycle software (Phoenix Flow Systems, San Diego, CA, USA). Mimosine synchronizations were performed as described (Krude, 1999): mimosine was added to growth media at 0.5 mM for 12–14 h, then cells were washed once with PBS and refed with fresh growth media lacking mimosine to initiate the cell cycle and S-phase.

Immunofluorescence microscopy

Immunofluorescence staining of cells with mouse anti-γH2AX (Upstate 05-636) and rabbit Thr68 phosphorylation-specific CHK2 (Cell Signaling, Beverly, MA, USA; no. 2661) antibodies was done according to manufacturer's recommendations. Secondary antibodies were Alexa 594-conjugated goat anti-rabbit (Molecular Dynamics, A11012) and FITC-conjugated donkey anti-mouse (Jackson Laboratories, West Grove, PA, USA; 715-095-151). The criteria for colocalization was the presence of both secondary antibody signals in the same nuclear volume of optical sections generated on the Zeiss Axiovert 200 confocal microscope. Image capture was done using a Zeiss Apotome digital camera and software. The best exposure time was determined for each channel and then used to acquire all subsequent images of optical sections. Images were exported as JPG files, opened in Adobe Photoshop and adjusted to a consistent image brightness prior to cropping to generate figures. No additional image processing was performed. The significance of differences in the frequency of colocalizing foci was determined by a χ^2-test employing 1 degree of freedom and Yates' correction.

Acknowledgments

We thank Dr. Brian Kennedy for use of his confocal microscope, and Alden Hackmann for graphics support. This work was supported by grants from the Nippon Boehringer Ingelheim Virtual Research Institute on Aging and the National Cancer Institute to R.J.M. Jr. This manuscript is dedicated to Dr. Robert W. Miller of the US National Cancer Institute, a Werner syndrome enthusiast, colleague and friend who died 23 February 2006.

References

d'Adda di Fagagna F, Reaper PM, Clay-Farrace L, Fiegler H, Carr P, von Zglinicki T, Saretzki G, Carter NP, Jackson SP (2003) A DNA damage checkpoint response in telomere-initiated senescence. *Nature* **426**, 194–198.

Ahn J, Urist M, Prives C (2004) The Chk2 protein kinase. *DNA Repair* **3**, 1039–1047.

Ahuja D, Sáenz-Robles MT, Pipas JM (2005) SV40 large T antigen targets multiple cellular pathways to elicit cellular transformation. *Oncogene* **24**, 7729–7745.

Bachrati CZ, Hickson ID (2003) RecQ helicases: suppressors of tumorigenesis and premature aging. *Biochem. J.* **374**, 577–606.

Bai Y, Murnane JP (2003) Telomere instability in a human tumor cell line expressing a dominant-negative WRN protein. *Hum. Genet.* **113**, 337–347.

Campisi J (2005) Senescent cells, tumor suppression, and organismal aging: good citizens, bad neighbors. *Cell* **120**, 513–522.

Chang S, Multani AS, Cabrera NG, Naylor ML, Laud P, Lombard D, Pathak S, Guarente L, DePinho RA (2004) Essential role of limiting

© 2006 The Authors
Journal compilation © Blackwell Publishing Ltd/Anatomical Society of Great Britain and Ireland 2006

telomeres in the pathogenesis of Werner syndrome. *Nat. Genet.* **36**, 877–882.

Courcelle J, Hanawalt PC (1999) RecQ and RecJ process blocked replication forks prior to the resumption of replication in UV-irradiated *Escherichia coli*. *Mol. Gen. Genet.* **262**, 543–551.

Crabbe L, Verdun RE, Haggblom CI, Karlseder J (2004) Defective telomere lagging strand synthesis in cells lacking WRN helicase activity. *Science* **306**, 1951–1953.

Dimri GP, Lee X, Basile G, Acosta M, Scott G, Roskelley C, Medrano EE, Linskens M, Rubelj I, Pereira-Smith O, Peacocke M, Campisi J (1995) A biomarker that identifies senescent human cells in culture and in aging skin *in vivo*. *Proc. Natl Acad. Sci. USA* **92**, 9363–9367.

Doe CL, Dixon J, Osman F, Whitby MC (2000) Partial suppression of the fission yeast *rqh1*$^-$ phenotype by expression of a bacterial Holliday junction resolvase. *EMBO J.* **19**, 2751–2762.

Du X, Shen J, Kugan N, Furth EE, Lombard DB, Cheung C, Pak S, Guangbin L, Pignolo RJ, Depinho RA, Guarente L, Johnson FB (2004) Telomere shortening exposes functions for the mouse Werner and Bloom syndrome genes. *Mol. Cell. Biol.* **24**, 8437–8446.

Ellis NA, Groden J, Ye T-Z, Straghen J, Lennon DJ, Ciocci S, Proytcheva M, German J (1995) The Bloom's syndrome gene product is homologous to RecQ helicases. *Cell* **83**, 655–666.

Epstein CJ, Martin GM, Schultz AL, Motulsky AG (1966) Werner's syndrome: a review of its symptomatology, natural history, pathologic features, genetics and relationship to the natural aging process. *Medicine* **45**, 177–221.

Gebhart E, Bauer R, Raub U, Schinzel M, Ruprecht KW, Jonas JB (1988) Spontaneous and induced chromosomal instability in Werner syndrome. *Hum. Genet.* **80**, 135–139.

Gebhart E, Schinzel M, Ruprecht KW (1985) Cytogenetic studies using various clastogens in two patients with Werner syndrome and control individuals. *Hum. Genet.* **70**, 324–327.

Goto M (1997) Hierarchical deterioration of body systems in Werner's syndrome: implications for normal ageing. *Mech. Ageing Dev.* **98**, 239–254.

Goto M, Miller RW, Ishikawa Y, Sugano H (1996) Excess of rare cancers in Werner syndrome (adult progeria). *Cancer Epidemiol. Biomarkers Prev.* **5**, 239–246.

Grandori C, Wu K-J, Fernandez P, Ngouenet C, Grim J, Clurman BE, Moser MJ, Oshima J, Russell DW, Swisshelm K, Frank S, Amati B, Dalla-Favera R, Monnat RJ Jr (2003) Werner syndrome protein limits Myc-induced cellular senescence. *Genes Dev.* **17**, 1569–1574.

Hearst JE, Isaacs ST, Kanne D, Rapoport H, Straub K (1984) The reaction of psoralens with deoxyribonucleic acid. *Q. Rev. Biophys.* **17**, 1–44.

Helleday T (2003) Pathways for mitotic homologous recombination in mammalian cells. *Mutat. Res.* **532**, 103–115.

Herbig U, Ferreira M, Condel L, Carey D, Sedivy JM (2006) Cellular senescence in aging primates. *Science* **311**, 1257.

Herbig U, Sedivy JM (2006) Regulation of growth arrest in senescence: telomere damage is not the end of the story. *Mech. Ageing Dev.* **127**, 16–24.

Herzing LBK, Meyn MS (1993) Novel *LacZ*-based recombination vectors for mammalian cells. *Gene* **137**, 163–169.

Hickson ID (2003) RecQ helicases: caretakers of the genome. *Nat. Rev Cancer* **3**, 169–178.

Hisama F, Chen Y-H, Meyn MS, Oshima J, Weissman SM (2000) WRN or telomerase constructs reverse 4-nitroquinoline 1-oxide sensitivity in transformed Werner syndrome fibroblasts. *Cancer Res.* **60**, 2372–2376.

Hoehn H, Bryant EM, Au K, Norwood TH, Boman H, Martin GM (1975) Variegated translocation mosaicism in human skin fibroblast cultures. *Cytogenet. Cell Genet.* **15**, 282–298.

Huang S, Lee L, Hanson NB, Lenaerts C, Hoehn H, Poot M, Rubin CD, Chen D-F, Yang C-C, Juch H, Dorn T, Spiegel R, Oral EA, Abid M, Battisti C, Lucci-Cordisco E, Neri G, Steed EH, Kidd A, Isley W, Showalter D, Vittone JL, Konstantoinow A, Ring J, Meyer P, Wenger SL, von Herbay A, Wollina U, Schuelke M, Huizenga CR, Leistritz DF, Martin GM, Mian IS, Oshima J (2006) The spectrum of *WRN* mutations in Werner syndrome patients. *Hum. Mutat.* **27**, 558–567.

Huschtscha LI, Thompson KVA, Holliday R (1986) The susceptibility of Werner's syndrome and other human skin fibroblasts to SV40-induced transformation and immortalization. *Proc. R. Soc. Lond. B, Biol. Sci.* **229**, 1–12.

Khakhar RR, Cobb JA, Bjergbaek L, Hickson ID, Gasser SM (2003) RecQ helicases: multiple roles in genome maintenance. *Trends Cell Biol.* **13**, 493–501.

Kipling D, Davis T, Ostler EL, Faragher RGA (2004) What can progeroid syndromes tell us about human aging? *Science* **305**, 1426–1431.

Kitao S, Shimamoto A, Goto M, Miller RW, Smithson WA, Lindor NM, Furuichi Y (1999) Mutations in *RECQ4L* cause a subset of cases of Rothmund–Thomson syndrome. *Nat. Genet.* **22**, 82–84.

Krude T (1999) Mimosine arrests proliferating human cells before the onset of DNA replication in a dose-dependent manner. *Exp. Cell Res.* **247**, 148–159.

Laud PR, Multani AS, Bailey SM, Wu L, Ma J, Kingsley C, Lebel M, Pathak S, DePinho RA, Chang S (2005) Elevated telomere-telomere recombination in WRN-deficient, telomere dysfunctional cells promotes escape from senescence and engagement of the ALT pathway. *Genes Dev.* **19**, 2560–2570.

Martin GM, Sprague CA, Epstein CJ (1970) Replicative life-span of cultivated human cells. Effects of donor's age, tissue, and genotype. *Lab. Invest.* **23**, 86–92.

Masuda T, Akasaka Y, Ito K, Ishikawa Y, Ishii T (2001) Pathology: Werner syndrome and normal aging. *Gann. Monograph Cancer Res.* **49**, 41–50.

Monnat RJ Jr (2001) Cancer pathogenesis in the human RecQ helicase deficiency syndromes. *Gann. Monograph Cancer Res.* **49**, 83–94.

Monnat RJ Jr (2002) Werner syndrome. In *WHO/IARC Monograph on Pathology and Genetics of Tumours of Soft Tissue and Bone* (Fletcher C, Unni K, Mertens F, eds), pp. 273–274. Lyon: IARC Press.

Monnat RJ Jr, Saintigny Y (2004) The Werner syndrome protein: unwinding function to explain disease. *Sci. Aging Knowl. Environ.* (13), re3.

Moser MJ, Kamath-Loeb AS, Jacob JE, Bennett SE, Oshima J, Monnat RJ Jr (2000) WRN helicase expression in Werner syndrome cell lines. *Nucl. Acids Res.* **28**, 648–654.

Oakley TJ, Hickson ID (2002) Defending genome integrity during S-phase: putative roles for RecQ helicases and topoisomerase III. *DNA Repair* **1**, 175–207.

Ogburn CE, Oshima J, Poot M, Chen R, Hunt KE, Gollahon KA, Rabinovitch PS, Martin GM (1997) An apoptosis-inducing genotoxin differentiates heterozygotic carriers for Werner helicase mutations from wild-type and homozygous mutants. *Hum. Genet.* **101**, 121–125.

Okada M, Goto M, Furuichi Y, Sugimoto M (1998) Differential effects of cytotoxic drugs on mortal and immortalized B-lymphoblastoid cell lines from normal and Werner's syndrome patients. *Biol. Pharm. Bull.* **21**, 235–239.

Opresko PL, Cheng W-H, Bohr VA (2004a) Junction of RecQ helicase biochemistry and human disease. *J. Biol. Chem.* **279**, 18099–18102.

Opresko PL, Mason PA, Podell ER, Lei M, Hickson ID, Cech TR, Bohr VA (2005) POT1 stimulates RecQ helicases WRN and BLM to unwind telomeric DNA substrates. *J. Biol. Chem* **280**, 32069–32080.

Opresko PL, Otterlei M, Graakjær J, Bruheim P, Dawut L, Kolvraa S, May A, Seidman MM, Bohr VA (2004b) The Werner syndrome helicase

© 2006 The Authors
Journal compilation © Blackwell Publishing Ltd/Anatomical Society of Great Britain and Ireland 2006

and exonuclease cooperate to resolve telomeric D loops in a manner regulated by TRF1 and TRF2. *Mol. Cell* **14**, 763–774.

Oshima J, Campisi J, Tannock TCA, Martin GM (1995) Regulation of *c-fos* expreession in senescing Werner syndrome fibroblasts differs from that observed in senescing fibroblasts from normal donors. *J. Cell. Physiol.* **162**, 277–283.

Pichierri P, Franchitto A, Mosesso P, Palitti F (2001) Werner's syndrome protein is required for correct recovery after replication arrest and DNA damage induced in S-phase of cell cycle. *Mol. Biol. Cell* **12**, 2412–2421.

Poot M, Gollahon KA, Emond MJ, Silber JR, Rabinovitch PS (2002a) Werner syndrome diploid fibroblasts are sensitive to 4-nitroquinoline-N-oxide and 8-methoxypsoralen: implications for the disease phenotype. *FASEB J* **16**, 757–758.

Poot M, Gollahon KA, Rabinovitch PS (1999) Werner syndrome lymphoblastoid cells are sensitivie to camptothecin-induced apoptosis in S-phase. *Hum. Genet.* **104**, 10–14.

Poot M, Silber JR, Rabinovitch PS (2002b) A novel flow cytometric technique for drug cytotoxicity gives results comparable to colony-forming assays. *Cytometry.* **48**, 1–5.

Poot M, Yom JS, Whang SH, Kato JT, Gollahon KA, Rabinovitch PS (2001) Werner syndrome cells are sensitive to DNA cross-linking drugs. *FASEB J* **15**, 1224–1226.

Prince PR, Emond MJ, Monnat RJ Jr (2001) Loss of Werner syndrome protein function promotes aberrant mitotic recombination. *Genes Dev.* **15**, 933–938.

Prince PR, Ogburn CE, Moser MJ, Emond MJ, Martin GM, Monnat RJ Jr (1999) Cell fusion corrects the 4-nitroquinoline 1-oxide sensitivity of Werner syndrome fibroblast cell lines. *Hum. Genet.* **105**, 132–138.

Saintigny Y, Makienko K, Swanson C, Emond MJ, Monnat RJ Jr (2002) Homologous recombination resolution defect in Werner syndrome. *Mol. Cell. Biol.* **22**, 6971–6978.

Saito H, Moses RE (1991) Immortalization of Werner syndrome and progeria fibroblasts. *Exp. Cell Res.* **192**, 373–379.

Salk D, Au K, Hoehn H, Martin GM (1985) Cytogenetic aspects of Werner syndrome. *Adv. Exp. Med. Biol.* **190**, 541–546.

Salk D, Au K, Hoehn H, Stenchever MR, Martin GM (1981) Evidence of clonal attenuation, clonal succession, and clonal expansion in mass cultures of aging Werner's syndrome skin fibroblasts. *Cytogenet. Cell Genet.* **30**, 108–117.

Smith JR, Pereira-Smith OM, Schneider EL (1978) Colony size distributions as a measure of *in vivo* and *in vitro* aging. *Proc.Natl Acad. Sci. USA* **75**, 1353–1356.

Swanson C, Saintigny Y, Emond MJ, Monnat RJ Jr (2004) The Werner syndrome protein has separable recombination and viability functions. *DNA Repair* **3**, 1–10.

Szekely AM, Bleichert F, Nümann A, Van Komen S, Manasanch E, Nasr AB, Canaan A, Weissman SM (2005) Werner protein protects nonproliferating cells from oxidative DNA damage. *Mol Cell Biol* **25**, 10492–10506.

Thiriet C, Hayes JJ (2005) Chromatin in need of a fix: phosphorylation of H2AX connects chromatin to DNA repair. *Mol. Cell* **18**, 617–622.

Wang LL, Gannavarapu A, Kozinetz CA, Levy ML, Lewis RA, Chintagumpala MM, Ruiz-Maldanado R, Contreras-Ruiz J, Cunniff C, Erickson RP, Lev D, Rogers M, Zackai EH, Plon SE (2003) Association between osteosarcoma and deleterious mutations in the RECQL4 gene in Rothmund–Thomson syndrome. *J Natl Cancer Inst.* **95**, 669–674.

Wyllie FS, Jones CJ, Skinner JW, Haughton MF, Wallis C, Wynford-Thomas D, Faragher RGA, Kipling D (2000) Telomerase prevents the accelerated cell ageing of Werner syndrome fibroblasts. *Nat. Genet.* **24**, 16–17.

Yu C-E, Oshima J, Fu Y-H, Wijsman EM, Hisama F, Alisch R, Matthews S, Nakura J, Miki T, Ouais S, Martin GM, Mulligan J, Schellenberg GD (1996) Positional cloning of the Werner's syndrome gene. *Science* **272**, 258–262.

Supplementary material

The following supplementary material is available for this article:

Fig. S1 8-Methoxypsoralen sensitivity of primary WS fibroblasts. (a–c) Proliferative survival of WS and control primary fibroblast strain pairs, matched for proliferative rate, over 72 h after 8-MOP+UV light treatment. Cell strain pairs were (a): 73-26 (W) and 71-95 (C); (b): AOMOR1010 (W) and 82-6 (C); and (c): AG00780G (W) and 78-89 (C). Error bars indicate standard deviations of triplicate experiments. These data have been re-analyzed and redrawn from data previously published in part (Poot *et al*., 2002a).

This material is available as part of the online article from:

http://www.blackwell-synergy.com/doi/abs/10.1111/j.1474-9726.2006.00260.x

(This link will take you to the article abstract).

Please note: Blackwell Publishing are not responsible for the content of functionality of any supplementary materials supplied by the authors. Any queries (other than missing material) should be directed to the corresponding author for the article.

© 2006 The Authors
Journal compilation © Blackwell Publishing Ltd/Anatomical Society of Great Britain and Ireland 2006